Renewable Energy 134 (2019) 1200–1212

Contents lists available at ScienceDirect

Renewable Energy

journal homepage: www.elsevier.com/locate/renene

Modeling diesel engine fueled with tamanu oil - Diesel blend by hybridizing neural network with firefly algorithm

Yarrapragada K.S.S Rao [a, *], B. Bala Krishna [b]

[a] Aditya College of Engineering, Andhra Pradesh 533437, India
[b] Jawaharlal Nehru Technological University, Kakinada, Andhra Pradesh 533003, India

A R T I C L E I N F O

Article history:
Received 12 March 2018
Received in revised form
3 August 2018
Accepted 28 August 2018
Available online 6 September 2018

Keywords:
Tamanu oil
Neural model
Firefly algorithm
Diesel engine
Biodiesel

A B S T R A C T

Research works are ongoing in mixing the biologically synthesized oil with the diesel for reducing the effect of global warming and climate change. From the review study, it is noted that the blended biodiesels require more assert about their practical viability. So, the non-edible Tamanu oil is synthesized and it is blended with diesel and its emission characteristics, engine performance and combustion characteristics are studied in our previous work. This paper attempts to model the diesel engine fueled with tamanu oil biodiesel blend. The proposed model exploits the context of neural network and the firefly algorithm is used to train it. After analyzing the various characteristics of the diesel engine, the acquired data is subjected to a proposed FF-NM method. The simulated results are statistically evaluated and the proposed modeling method is proved to be better than the other NM.

1. Introduction

Gradual reduction of the crude oil and the recent climatic changes paves the way for the identification of any other fuels. Specifically, in recent years, the biofuels are considered most because of its renewable capacity. The environment gets polluted due to the emission of GHG and other toxic gases from the diesel engine of vehicles. Researchers paid attention to minimize the emission of poisonous gases that cause lot of side effects and developed new methodologies.

Biodiesel is a nontoxic and biodegradable fatty acid methyl ester [11]. It is obtained from the renewable resource and it is completely a nonconventional fuel with no petroleum components and it is synthesized from the vegetable oil or waste greases or animal fats or feed stocks having triglycerides using the process of trans-esterification [13,16]. The oils from the plants and animals are either edible or non-edible and the edible oils are less used for the biodiesel production because of the high price of an edible oil [12,17] [18]. So, the non-edible oils are used for the synthesis of biodiesel and it is used as a fuel in the diesel engine. One such non-edible oil is the TO, obtained from the *Calophyllum inophyllum* seeds that are frequently seen in the tropical areas. The unrefined TO consist of about 22% FFA [14] and this low amount of free fatty acids is a good property for the production of biodiesel because high amount of FFA lead to the generation of soap with addition of alkaline catalyst [15]. The steps involved in the production of biodiesel are pretreatment, acid-catalysed esterification and acid catalysed alkylation. The produced biodiesel is blended with the pure diesel for its use in engine to reduce the emissions of the GHG [6]. The blended form of biodiesel is supplied to the engine and trialled at varied compression ratios in a diesel engine and the output is evaluated by analysing the characteristics of the combustion, performance and emission in the engine. The property of inferior oxidative and the storage stability [19,20] are the limitations of the use of biodiesel.

The main contribution of this paper is to model the diesel engine with blended fuels like tamanu oil and biodiesel in order to reduce the effect of global warming and climate change. The proposed model utilizes the context of neural network and the firefly algorithm is exploited to train it. After analyzing the various characteristics and features of the diesel engine, the data is presented to a proposed FF-NM method.

2. Literature review

2.1. Tamanu oil based biodiesel blends

In 2011, Selvebala et al. [7] applied the response surface

* Corresponding author.
E-mail addresses: subbaraoyks123@gmail.com (Y. K.S.S Rao), balakrishnajntu06@gmail.com (B. Bala Krishna).

https://doi.org/10.1016/j.renene.2018.08.091
0960-1481/

Abbreviation description

FF-NM	Firefly-neural model
GHG	Green house gases
TO	Tamanu oil
FFA	free fatty acid
NLARX	The non-linear autoregressive exogenous input
MSE	The Mean square error
CR	Compression Ratio
BMEP	Brake Mean Effective Pressure
IP	Induction Point
IMEP	Indicated Mean Effective Pressure
SFC	specific fuel consumption
BP	Brake Power
AF ratio	Air Fuel ratio

methodology and the central composite design for identification of the optimized process of operation in the pre-treatment step and they optimized the process of pre-treatment in beta-zeolite modification in acid. In 2014, Gnanomoorthi and Devaradjane [4] utilized the ethanol blended diesel oil by adding 1% Diethyl Carbonate and 1% ethyl Acetate as the biofuel for the experimental study and evaluated the combustion, emission and the performance in four stroke, one cylinder, direct injection aspirated diesel engine with varied compression ratios. Fattah et al. [8] studied the emission and performance in a four cylinder diesel engine with the TO that is subjected to esterification process with the addition of Potassium Hydroxide, Sulphuric acid and antioxidants. The results showed the efficiency of the developed blend ratio with reduction in brake specific fuel and increase in brake power.

In 2015, Kumar et al. [6] have worked on the esterified pinnai oil and studied the performance and the emission characteristics with varied compression ratios in a diesel engine. They specifically considered various parameters such as temperature, time, pH, the amount of catalyst added is considered with respect to the production of biodiesel and the brake specific energy consumption, brake thermal efficiency, combustion duration, ignition delay and exhaust gas temperature is considered in studying the efficiency of the proposed blend ratios in a diesel engine. Bapu et al. [9] concentrated on the problem of emission of gases such as Carbon monoxide, hydrocarbon and smoke and so, done the experiment with mixed methyl ester of TO with diesel. The experiment is carried out in one cylinder with varied compression ratios and modified hemispherical combustion chamber. The simulation experiments are done using the Ansys Fluent software. Muthukumaran et al. [10] synthesized the *Calophyllum inophyllum* oil in modified form with the addition of catalyst – raw fly ash and had done the experiment in a diesel engine with one cylinder. The modified form of the TO is characterized using the techniques such

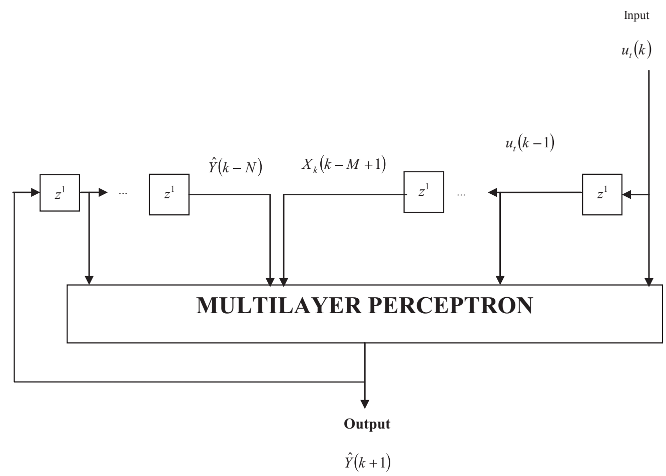

Fig. 2. Architecture of nonlinear autoregressive neural model.

Table 1
Engine specifications.

Particulars	Specifications
Engine make	Kirloskar TV-1
Number of cylinder	Single
Number of stroke	Four
Bore and Stroke length	87.5 mm and 110 mm
Power and speed	3.5 kW and 1500 rpm
Compression ratio	Varying range of 15, 16, 17 and 17.5
Swept volume	661.45 cc
Connecting rod length	1 mm

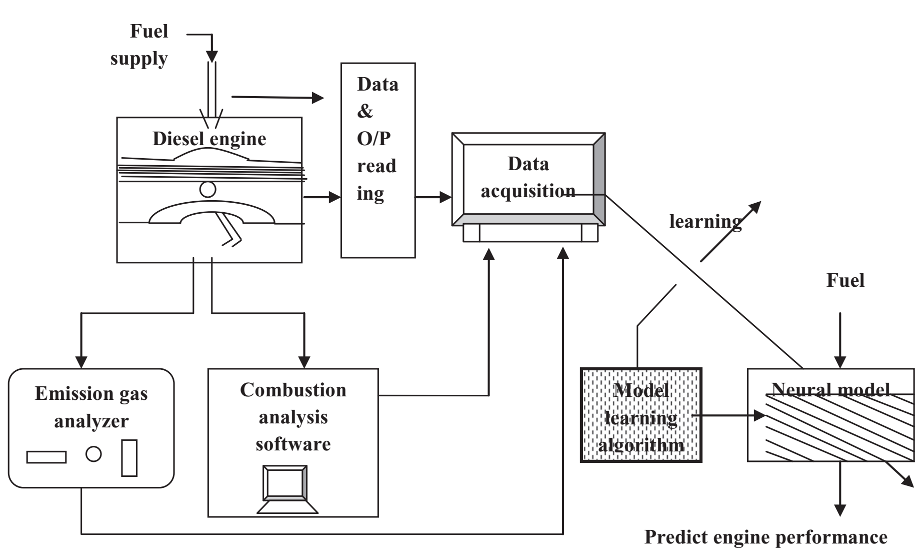

Fig. 1. Procedure to model a diesel engine for its engine performance and emission analysis.

as scanning electron microscopy and Electron dispersive x-ray spectroscopy and also, analysed the effects of the blended oil with the emission and performance of the diesel engine.

2.2. Other biodiesel blends

In 2015, Nagaraja et al. [3] blended the diesel with the preheated palm oil and experimentally worked out the effects of the blended oil with diesel engine considering the different compression ratios, the emission and the performance characteristics. The palm oil is subjected to 90 °C before the blending process and the parameters used for the simulation study includes the mechanical efficiency, brake power, and indicated mean effective pressure. From the results obtained, it was found that the emission of carbon monoxide and hydrocarbon is highly reduced with increased blend ratio and compression ratio. Senthil et al. [5] estimated the various effects of using Annona methyl ester as fuel in the diesel engine efficiency with varied compression ratios and considering parameters such as brake thermal efficiency, fuel injection timing and emission of carbon monoxide and hydrocarbon. In 2016, Bora and Saha [1] used the rice bran oil and blended with the diesel oil and studied the effect of this blended oil on the performance, emission and combustion characteristics in a diesel engine that is with biogas. So, the dual fuel run diesel engine consisting of one cylinder, naturally aspirated, water cooled, direct injection engine is run with selected compression ratios and the parameters such as maximum liquid replacement and the brake thermal efficiency are used as the measure for analysing the engine efficiency. Bora and Saha [2] have worked on the biogas run dual fuel diesel engine and introduced an optimization process for the pilot fuel injection timing and the

Table 2
Weight (ω) of NM and FF-NM for CO, HC, CO_2, O_2 and NO_X.

Weight ω	CO		HC		CO_2		O_2		NO_x	
	NN	FF-NM	NN	FF-NM	NN	FF-NM	NN	FF-NM	NN	FF-NM
1	−2.9439	4.6659	1.5326	0.64758	2.5904	−2.1046	0.9366	2.4074	0.9366	2.4074
2	−4.2811	2.0771	9.2872	−2.6684	−0.56686	−2.7368	−1.7816	0.017706	−1.7816	0.017706
3	1.4915	2.509	0.073924	−9.3876	0.31501	5.5258	4.678	8.339	4.678	8.339
4	0.68465	1.0443	2.7027	−1.7075	5.1889	5.8095	1.8042	0.76649	1.8042	0.76649
5	−1.7296	−0.54878	−1.1166	0.72636	6.8843	−6.7549	−1.0087	3.4243	−1.0087	3.4243
6	0.46546	−0.10591	−3.9051	0.81367	−3.2999	0.66171	−0.8304	0.29871	−0.8304	0.29871
7	1.0801	−1.7166	0.71614	0.5738	3.2308	−1.4759	2.9007	−3.6686	2.9007	−3.6686
8	0.62571	−2.0788	2.727	−8.208	−5.9361	4.6628	−2.2933	0.26886	−2.2933	0.26886
9	3.2425	−2.6149	2.0611	0.85462	0.17337	11.328	6.0863	−2.3034	6.0863	−2.3034
10	−2.6867	−3.0931	0.98328	−5.2515	−3.6781	−2.3815	−4.6223	2.6164	−4.6223	2.6164
11	1.1129	0.23314	−1.1945	−0.037154	0.47571	0.23307	0.11478	−0.21293	0.11478	−0.21293
12	0.021546	−1.7865	0.5559	−1.8608	0.12827	0.77734	−0.16504	−0.053749	−0.16504	−0.053749
13	0.92041	−1.1697	−0.50454	−0.98055	0.097213	0.096377	−0.13686	−3.5442	−0.13686	−3.5442
14	−0.78027	−2.4808	0.1432	−0.69313	0.38786	−0.28529	−0.0061194	−0.23846	−0.0061194	−0.23846
15	1.8761	−0.44422	0.2545	−0.89935	−0.2813	3.1199	−0.069643	−0.4518	−0.069643	−0.4518
16	−0.58158	1.1904	−0.23117	0.10227	−0.50085	1.4482	−0.093121	−0.37314	−0.093121	−0.37314
17	1.1061	−0.75392	0.39499	0.19118	−0.56951	−0.4149	−0.010368	0.42048	−0.010368	0.42048
18	−0.4063	−1.6262	0.036618	−0.84285	−0.36757	−2.4917	−0.063388	0.42186	−0.063388	0.42186
19	0.15544	−0.44182	−0.18183	−1.8477	−0.1168	1.5093	−0.28183	−0.48323	−0.28183	−0.48323
20	−2.3155	−2.8022	0.02392	−1.2639	−0.47239	−2.8531	0.30093	0.91599	0.30093	0.91599
21	1.3533	−2.8609	2.3424	−0.87046	2.9383	−0.40408	1.0878	1.8898	1.0878	1.8898
22	2.7862	−0.6914	−5.4342	1.0999	−0.56496	−0.76099	−2.0416	1.0516	−2.0416	1.0516
23	−0.36844	−0.68055	−0.3585	4.2206	0.56326	−5.6874	−5.8846	−4.6708	−5.8846	−4.6708
24	−2.0641	0.97168	−3.6141	1.259	−5.9828	−5.7206	−2.729	1.6799	−2.729	1.6799
25	−0.6982	0.28127	−2.0368	1.1575	−7.2729	0.91556	1.0156	−5.5292	1.0156	−5.5292
26	1.2964	−1.1679	5.9054	−2.0979	1.9917	−0.79808	2.548	−1.5259	2.548	−1.5259
27	0.63488	−2.6247	1.6861	1.0317	−4.0305	0.30224	−4.685	5.9836	−4.685	5.9836
28	1.5335	−1.0142	−3.1432	2.8946	7.7128	−3.0536	4.3011	−1.5771	4.3011	−1.5771
29	−2.681	−1.3669	2.5044	0.79511	0.048228	−13.051	−7.6171	1.9756	−7.6171	1.9756
30	1.2481	−0.089864	2.761	7.1909	3.241	−0.31536	3.9511	−1.7115	3.9511	−1.7115
31	3.0007	2.0796	−1.6486	−0.20779	−0.065393	−1.9947	0.076742	−1.3179	0.076742	−1.3179
32	−2.0693	1.5221	3.6329	−2.665	−0.26531	−5.301	0.20863	0.031811	0.20863	0.031811
33	2.9193	2.8576	−0.87234	−6.5784	−0.30915	1.4715	0.16375	6.3604	0.16375	6.3604
34	1.575	−0.98907	0.44871	1.6112	0.96626	0.47093	0.036481	−0.45552	0.036481	−0.45552
35	−0.23565	−1.6654	0.27142	−1.0985	0.25192	9.8167	0.25749	−1.5511	0.25749	−1.5511
36	0.6701	−2.4947	−0.79711	0.015657	−2.4307	−0.79777	−0.20305	0.1698	−0.20305	0.1698
37	−2.6841	−0.86269	0.64223	−0.041489	0.018311	−0.12619	0.75777	1.8565	0.75777	1.8565
38	−2.6224	1.4637	−0.21881	−5.722	−0.34252	−6.7687	0.17182	−1.3109	0.17182	−1.3109
39	2.029	−2.4147	−0.41134	−2.615	0.32455	2.0907	0.61904	0.26097	0.61904	0.26097
40	1.6538	0.67353	−0.13685	−3.5102	−1.3031	1.0064	−0.25242	−0.67582	−0.25242	−0.67582
41	0.83268	1.2162	4.3089	2.7645	−4.3718	−5.9488	−1.5546	1.0764	−1.5546	1.0764
42	−1.2646	−1.6853	−3.085	4.4731	3.8726	−0.51746	3.9384	−0.44854	3.9384	−0.44854
43	2.6594	0.62306	−6.6147	0.022442	−5.1786	−0.10657	1.7879	3.9463	1.7879	3.9463
44	0.9471	−0.61632	0.97496	−1.7814	−4.572	−7.5072	−9.0779	−2.9777	−9.0779	−2.9777
45	0.1536	0.14657	−2.831	0.027803	−13.706	10.545	26.151	−1.1336	26.151	−1.1336
46	−0.14102	−0.98434	−12.409	3.5996	8.1829	−0.15265	−8.0679	2.4135	−8.0679	2.4135
47	0.35771	0.067285	−0.9391	−1.2914	1.6255	−0.23453	8.0483	0.75024	8.0483	0.75024
48	−0.02671	−0.24414	−4.3167	−2.3254	3.0213	−3.9789	−2.2864	2.0894	−2.2864	2.0894
49	−0.10528	0.2806	4.2933	6.514	−3.0278	−0.38652	7.5871	0.46231	7.5871	0.46231
50	1.0767	0.060871	−3.0044	−1.5347	−7.1889	−1.0324	2.9055	−3.7307	2.9055	−3.7307
51	−0.083673	−0.072467	−3.0468	−0.06691	8.8013	0.090339	8.1638	−0.83498	8.1638	−0.83498
52	−2.9439	4.6659	1.5326	0.64758	2.5904	−2.1046	0.9366	2.4074	0.9366	2.4074

Table 3
MSE between the actual and predicted engine performance of the diesel engine fueled with tamanu oil blend.

Parameters (units)	CR15		CR16		CR17		CR17.5	
	NM	FF-NM	NM	FF-NM	NM	FF-NM	NM	FF-NM
Torque (N.m)	2.44	1.12	1.92	1.30	1.56	0.62	2.41	0.0070
BP(Kg/kW.s)	0.00044	4.6062e-05	0.00041	5.3657e-05	0.022	0.020	0.0077	0.016
IP(kW)	1.12	0.37	0.32	0.06	0.40	0.11	5.16	2.14
BMEP(N/m^2)	0.02	0.0027	0.06	0.0035	0.04	0.02	0.014	0.0039
IMEP(N/m^2)	9.95	4.65	1.08	0.59	0.059	0.01	1.50	1.01
BTHE (W.s/J)	0.20	0.18	1.06	0.043	4.21	3.71	0.054	0.027
ITHE (W.s/J)	1794.2	1046.8	406.65	29.04	52.59	32.70	127.51	117.72
Mechanical efficiency	37.03	25.25	222.15	38.38	410.83	20.006	351.95	159.06
Air flow (Kg/s)	0.097	0.023	0.04	0.0052	0.0091	0.0078	0.044	0.00066
Fuel flow (Kg/s)	0.00027	0.00020	0.00030	2.1947e-05	0.0023	0.00030	0.00021	0.00016
SFC(Kg/J)	0.24	0.12	0.024	0.013	0.15	0.05	0.08	0.010
Volume efficiency (1/rev)	0.069	0.0031	0.0043	0.0023	0.095	0.039	0.06	0.05
AF ratio	31.68	21.42	42.13	14.85	448.86	96.97	127.33	8.5
HBP (%)	0.22	0.16	1.78	0.29	2.37	2.29	0.084	0.032
HJ (%)	4.72	2.88	16.02	307.01	252.34	741.93	3.23	11.47
HGas (%)	0.80	0.50	6.32	1.59	4.90	1.91	2.45	1.40
HRad (%)	18.51	2.651	25.43	21.32	229.18	85.45	33.65	20.37

compression ratios. They proposed this optimization method to overcome the odd effect of the engine and the surroundings and the method shows very less emission of the carbon monoxide and the hydrocarbons.

3. Modeling of diesel engine

3.1. System model

The schematic representation of the system model is shown in Fig. 1. The blended fuel-TO-diesel oil is supplied to the Kirloskar SV1 model diesel engine having water cooled, directly injected, four stroke one cylinder. The engine works at a speed of 1500 rpm and generates a power of 5.2 kW. The system model also consists of the emission gas analyzer and the combustion analysis systems for analysing the emission of gases CO, CO_2, O_2, NO_x, HC and for analysing the specific gas constant, air density, adiabatic index, cylinder pressure, polytrophic index respectively. The analysed data are read and recorded in O/P reading measurements. The data is collected and it is subjected to the model learning algorithm through the neural model and the model predicts the combustion characteristics, emission performance and the engine performance.

3.2. Autoregressive neural model

NLARX [25] model structure is one of the commonly used architecture style and its structure is depicted in Fig. 2.

Let $X(k)$ be the inputs and $Y(k)$ be the outputs and the NLARX model can be represented as:

$$Y(k) = F(Y(k-1), ..., Y(k-N), X(k), ...X(k-M=1)) \quad (1)$$

where, N and M represents the number of past output terms and input terms respectively that are used for predicting the current output. The generated outputs from the NLARX model are the conversion of the earlier inputs and outputs, which are actually the regressor functions having two types of blocks-linear and nonlinear block. The conventional regressors are due to the delayed output or input variables but, the advanced regressors exist in the arbitrary user defined function form of delayed output and input variables. So, the problem in NLARX model training can be a non linear unconstrained optimization issue and it is given as

$$\min_{\omega} e(\omega, z_T) = \frac{1}{2T}\sum_{t=1}^{T}\left\|Y_t(k) - \hat{Y}_t\ (k|\omega)\right\|^2 \quad (2)$$

where, $Z_T = [Y_t(k), X(k)]k = 1, ..., T$, $Y_t(k)$, $Y_t(k)$, $\hat{Y}_t\ (k|\omega)$, $\omega(\omega = [\omega_1, ..., \omega_i, ..., \omega_p])$, $\| \bullet \|^2$ and p represents the training data set, the output which is measured in the training set, output of NLARX, vector parameter, 2 norm operation and number of parameters respectively. In the neural network given in equation (1), there exists a, error metric called as the performance index of the equation (2) and it is important to minimize this index to overcome the metric error. The index also shows the network approximation to some given training patterns and the network parameters ω have to be modified to minimize the index $e(\omega, z_T)$ above the complete trajectory for obtaining the less value.

The model parameters given in the Table 2 represents the optimal weights of the NLARX model, which can correlate precisely with the experimental data. These weights are adopted as 'omega' in the model, which is given in eqs. (3) and (4), where b and c indicates the value 1.

$$Y_K(\omega = 1|\omega_{<i}) = sigm\left(b_i + \left(W^T\right)_i \bullet h_i\right) \quad (3)$$

$$h_i = sigm(c + W_{<i\omega<i}) \quad (4)$$

3.3. Firefly algorithm based learning process

FA [21,22,24]is proposed in 2007–2008 based on the behaviour and flashing patterns of the fireflies by Xin-She Yang at Cambridge University. It follows three rules, (1) With respect to the sex, the fireflies are unisex and so, one firefly will attract the other firefly, (2) The amount of attractiveness is proportional to the amount of brightness and automatically, the brightness and attractiveness decrease with respect to the distance and among the two flashing fireflies, the brightness less firefly move towards the more brightness firefly. In absence of a brighter firefly, they start the random move and (3) the landscape of the objective function determines the fireflies' brightness.

Since, the attractiveness of the firefly is proportional to the intensity of the light viewed by the nearby fireflies, the change in attractiveness expressed in β in distance r, is given as

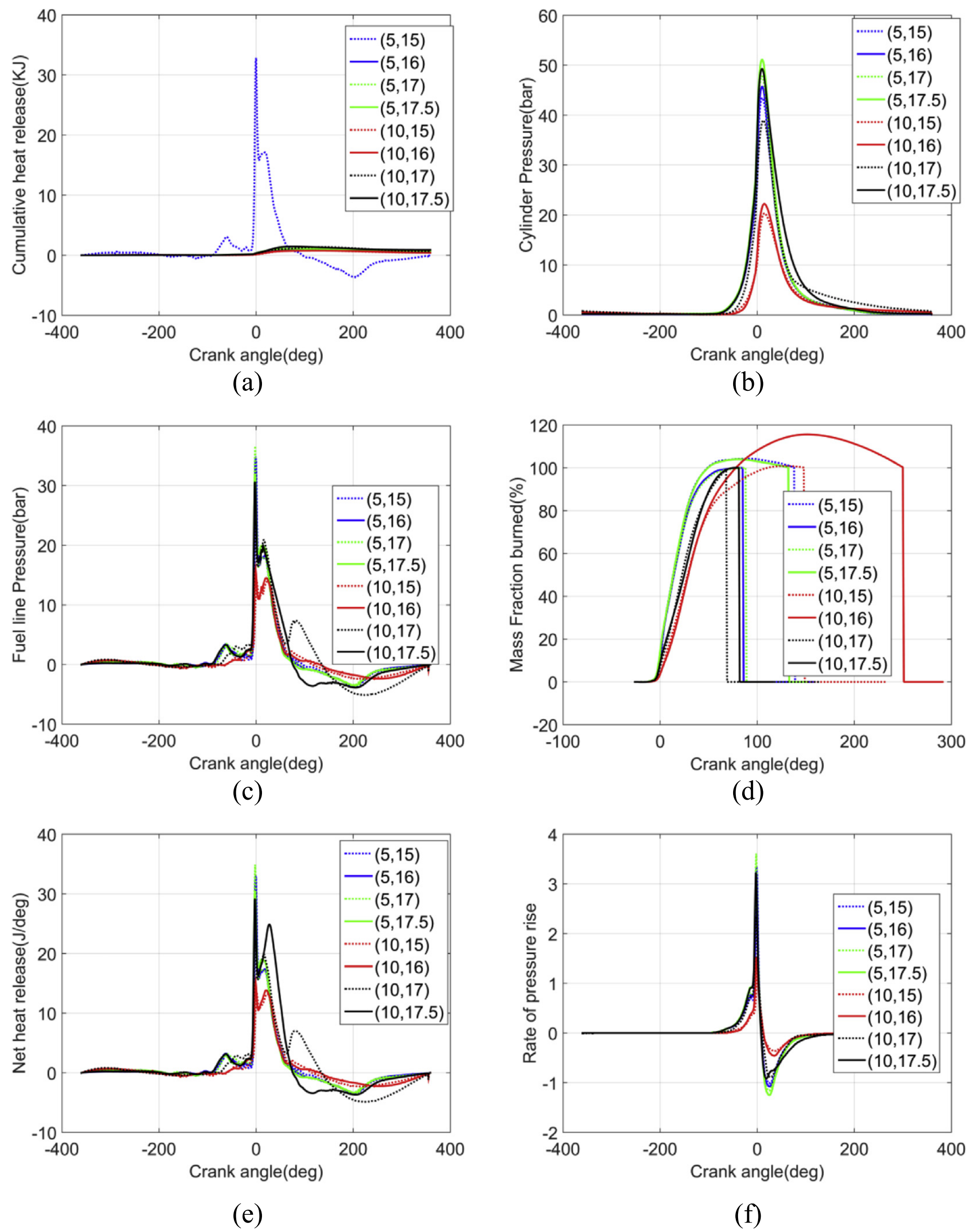

Fig. 3. Effect of compression ratio and blend ratio on the combustion characteristics of the diesel engine.

$$\beta = \beta_0 e^{-\gamma r^2} \tag{5}$$

where, β_0 represents the attractiveness at $r = 0$. If the firefly i which is in movement is attracted to the brighter firefly j, then

$$x_i^{t+1} = x_i^t + \beta_0 e^{-\gamma r_{ij}^2}\left(x_j^t - x_i^t\right) + \alpha_t \in_i^t \tag{6}$$

where, the second term is because of the attraction among the fireflies and the third term is in randomization with α_t, where, α_t is the parameter for randomization and $\in_i^t$ represents the randomly selected numbers using the Gaussian or uniform distribution at a time period t. The simple random walk may occur, when $\beta_0 = 0$ and when $\gamma = 0$, it gets minimized to a variant of Particle Swarm Optimization [21]. In addition to this, the $\in_i^t$ randomization will move towards the other distribution like Levy flights [21].

4. Experimental setup

4.1. Procedure

The experiment involves the use of one diesel engine supplied with the TO-diesel oil blends with varied compression ratios-15, 16, 17 and 17.5. The selected blend ratio (TO: diesel) are 5:95, 6:94, 7:

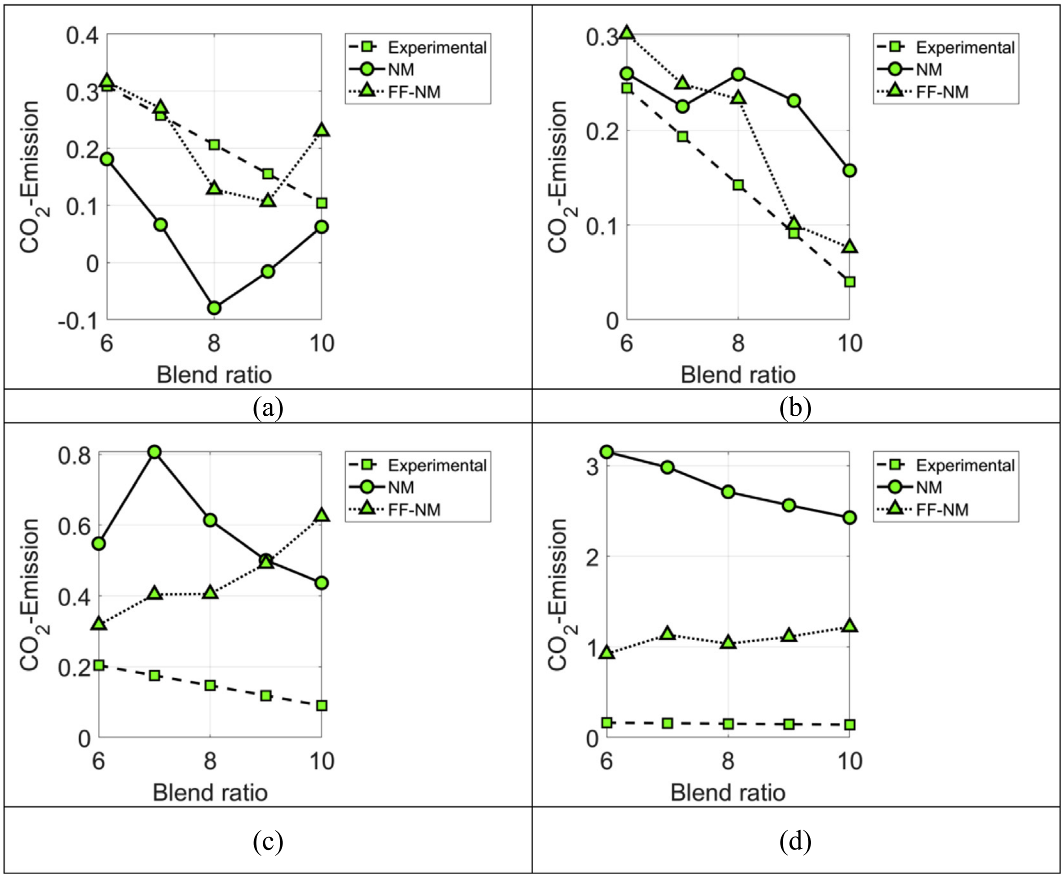

Fig. 4. Statistical interpolation of miniature blends for CO_2 under varying compression ratio of (a) 15, (b) 16, (c) 17, (d) 17.5.

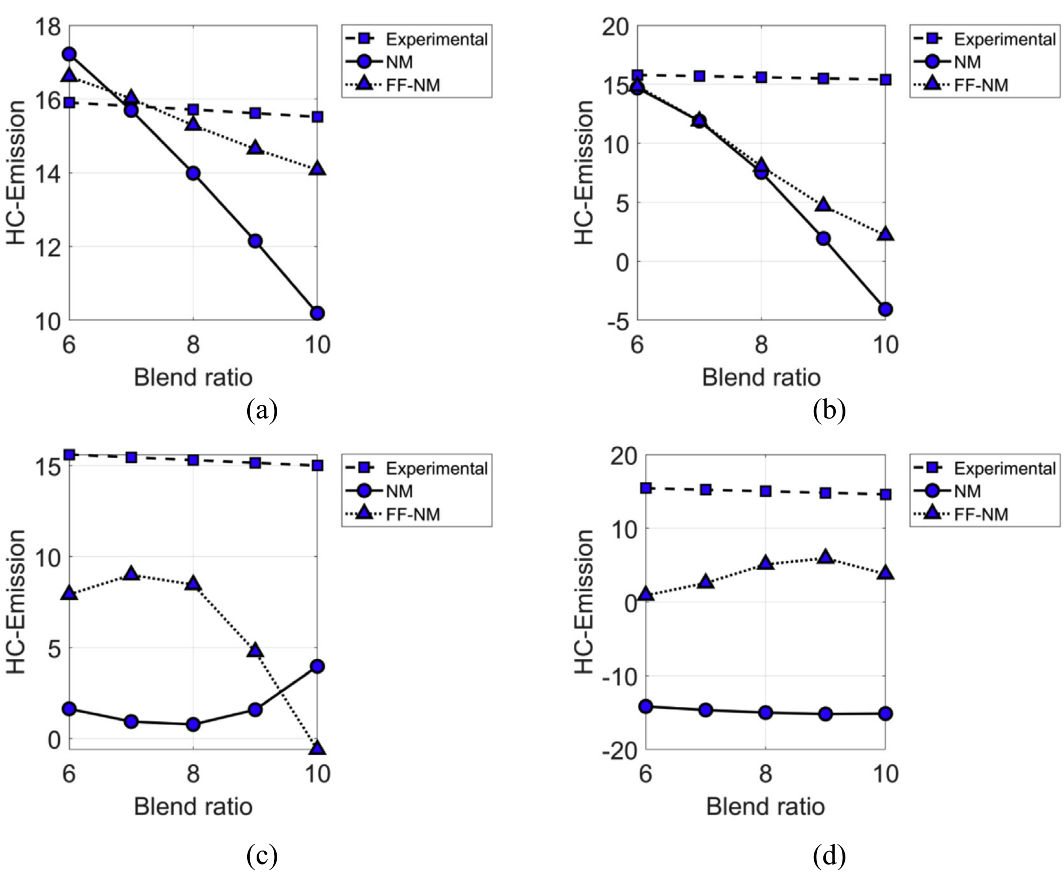

Fig. 5. Statistical interpolation of miniature blends for HC under varying compression ratios of (a) 15, (b) 16, (c) 17, (d) 17.5.

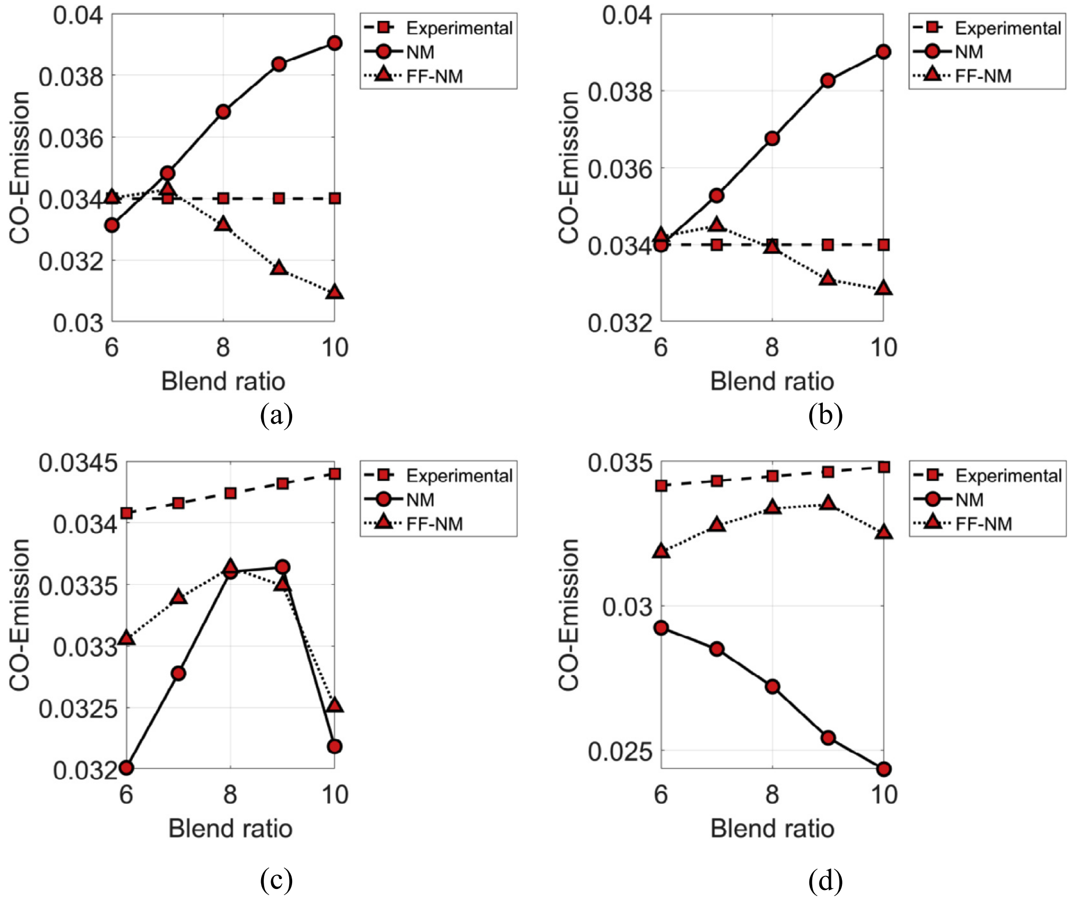

Fig. 6. Statistical interpolation of miniature blends for CO under varying compression ratios of (a) 15, (b) 16, (c) 17, (d) 17.5.

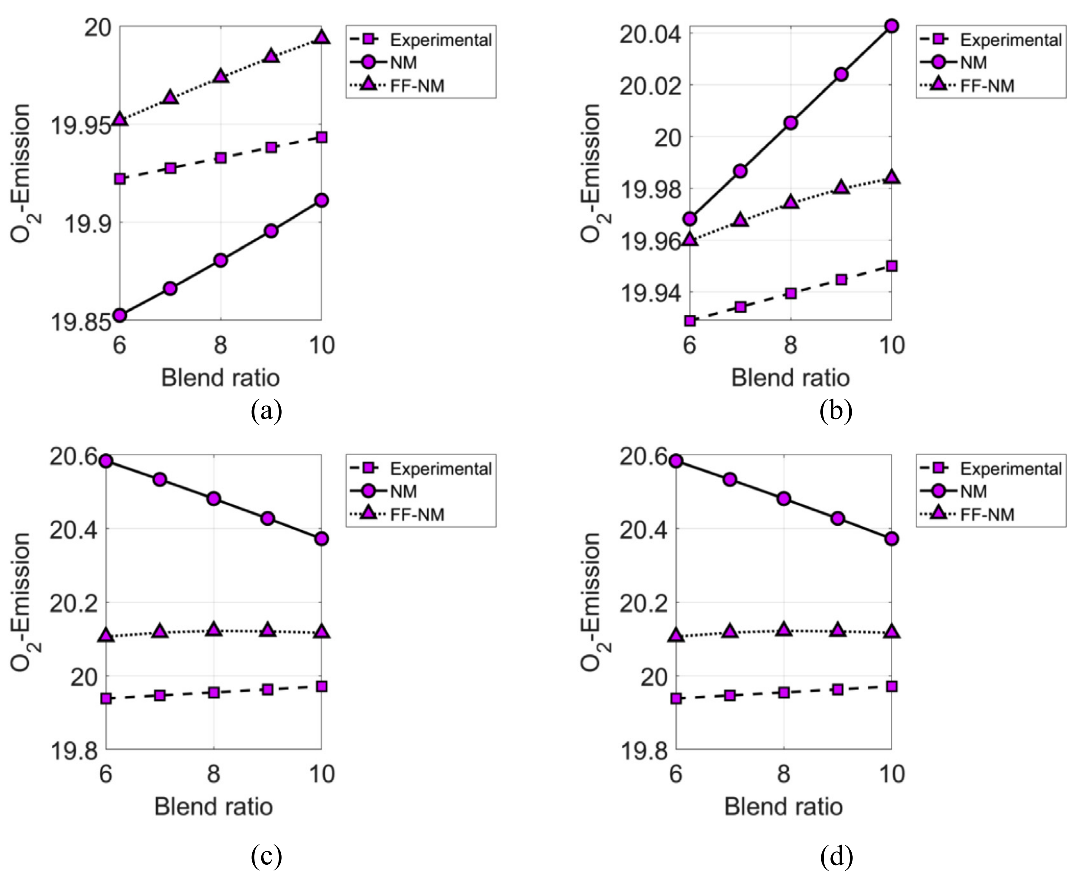

Fig. 7. Statistical interpolation of miniature blends for O_2 under varying compression ratios of (a) 15, (b) 16, (c) 17 (d) 17.5.

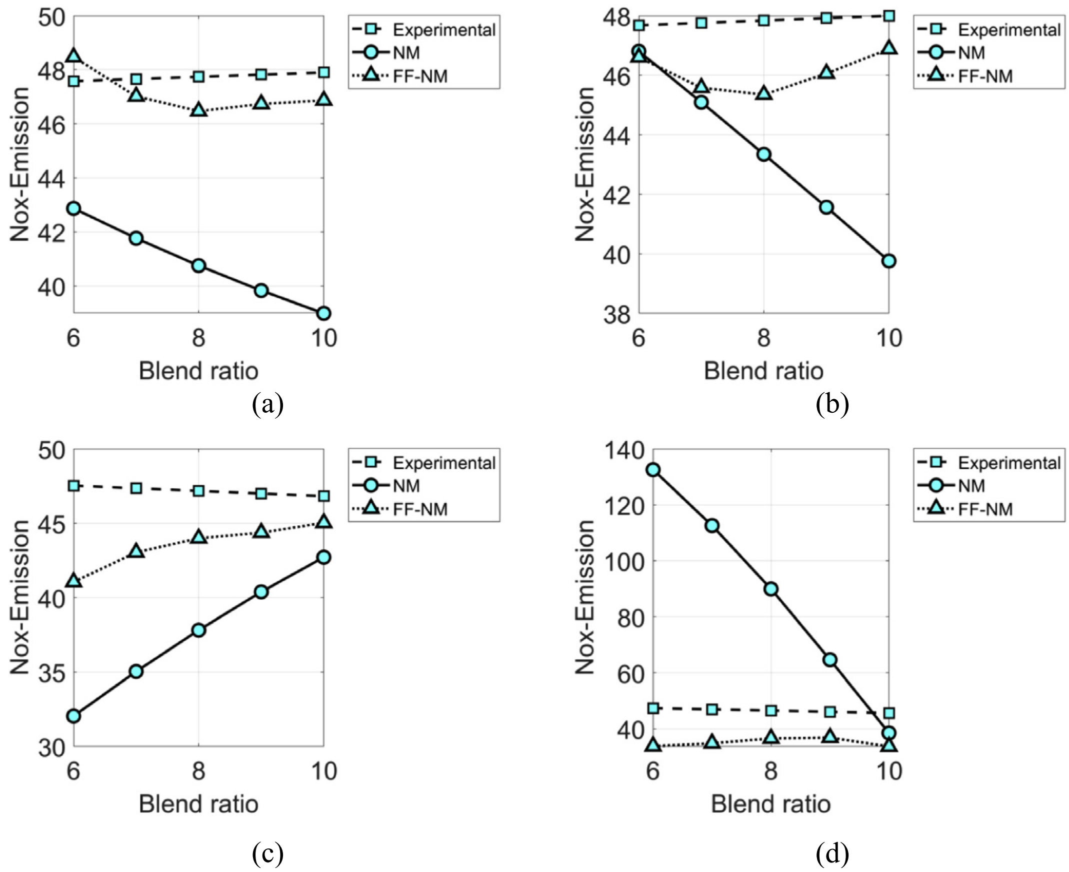

Fig. 8. Statistical interpolation of miniature blends for NO_x under varying compression ratios of (a) 15, (b) 16, (c) 17, (d) 17.5.

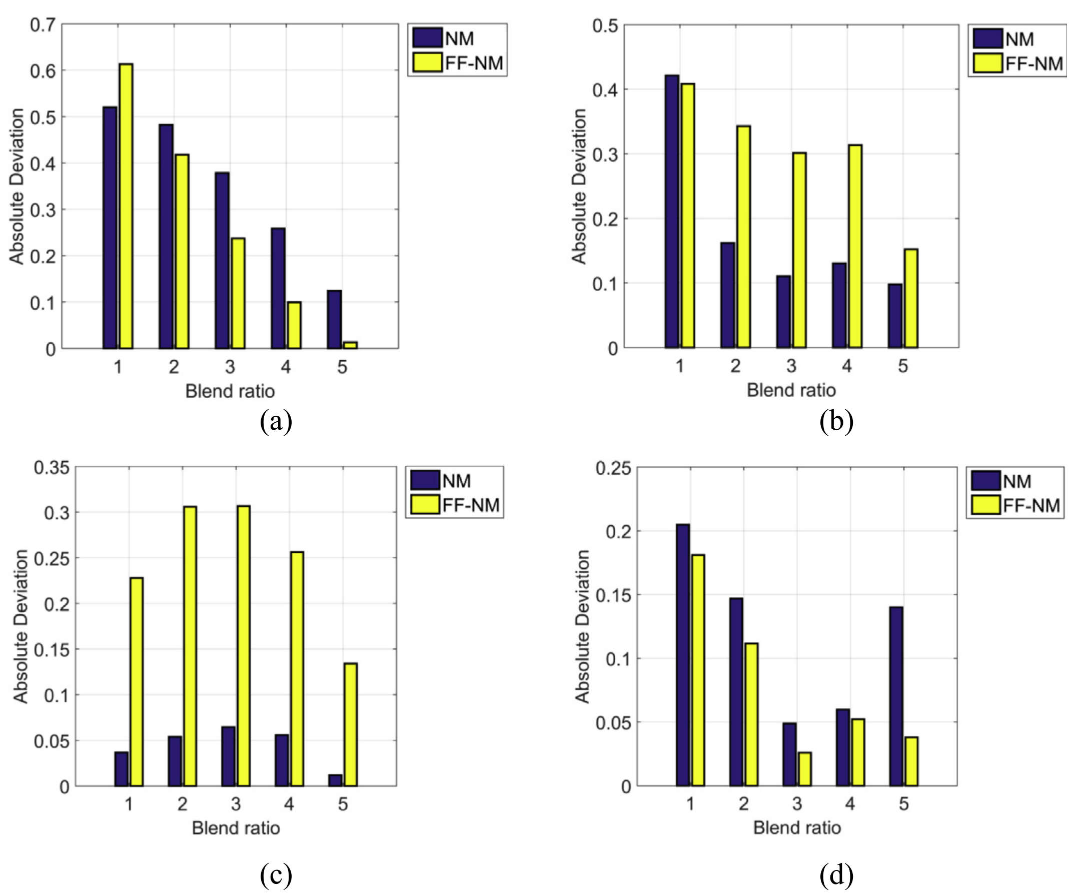

Fig. 9. Absolute deviation of miniature blends of CO_2 for the proposed FF-NM method over NM method under varying compression ratios of (a) 15, (b) 16, (c) 17, (d) 17.5.

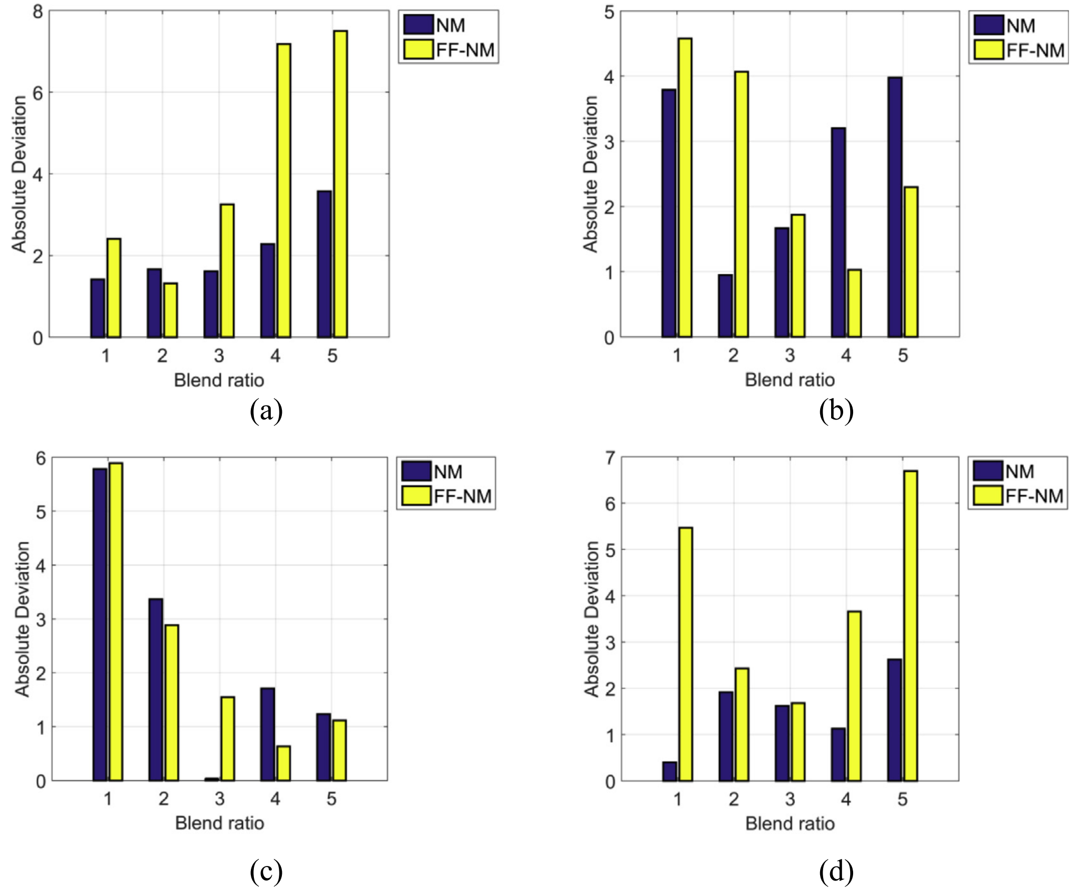

Fig. 10. Absolute deviation of miniature blends of HC for the proposed FF-NM method over NM method under varying compression ratios of (a) 15, (b) 16, (c) 17, (d) 17.5.

93, 8:92, 9:91, and 10:90 and all the parametric measures, the performance and the emission values are recorded. The acquired data is used to simulate the neural model - Levenberg Marquadt [23] learning algorithm. This algorithm is a traditional one and it has various limitations such as regularization problem and overfitting. So, a new neural model is proposed and it is trained by recently introduced firefly algorithm. The experiments were carried out and the results are tabulated and interpreted in the following section. The specifications of the engine used for our experimental study is cited in Table 1.

The MSE between actual and predicted engine performance of the diesel engine with 6%, 7%, 8%, 9%, 10% TO blend with varied compression ratio 15, 16, 17 and 17.5 is noted in Table 3. Various parameters are considered for predicting the engine performance. The parameters include Torque, BP, IP, BMEP, IMEP, BTHE, ITHE, Mechanical efficiency, air flow, fuel flow, SFC, volume efficiency, AF-ratio, HBP, HJW, HGas, and HRad. The MSE is determined between the actual and the predicted outcome from NM and FF-NM methods. The MSE of all the predicted parameters from FF-NM model is relatively less even with variations of CRs and blend ratios except the parameter BP at CR 17.5 and HJ at CR 16, 17, 17.5. The increase in MSE than the NM cannot be significant because of such negative deviation only at few instants and minimum deviation. The best performance among the parameters for the proposed FF-NM method is found to be the Torque at CR 17.5 having a MSE deviation of 99.7% over NM. In the mechanical efficiency parameter, the MSE of FF-NM method deviates 82.7%, 95.13% and 54.8% over existing NM method for the corresponding CR of 16, 17 and 17.5.

The combustion characteristics with respect to the different CRs are evaluated with the TO-diesel blend 5% and 10%. The combustion parameters like fuel line pressure, mass fraction burned, cylinder pressure, net heat release, cumulative heat release and rate of pressure rise are analysed using the combustion analysis software and it is shown in Fig. 3. Fuel line pressure indicates the pressure of the fuel measured at the fuel line in a given rated speed. Mass fraction burned combustion parameter calculates from the percentage of fuel to be burned out of the total mass of fuel. Net heat release parameter represents the volume of heat released during the combustion of a specified amount of fuel and Rate of pressure rise combustion parameter is defined as the expansion of high-pressure gases produced by applying direct force to some component of the engine. Other combustion parameters such as cumulative heat release and cylinder pressure states the total energy released as heat when a fuel undergoes complete combustion with oxygen under standard conditions and the pressure in engine cylinder during the 4 strokes of engine operation respectively.

In the initial phase of the blending, the pressure rate increases because of the mixed fuels intensity. When the CR is 17.5 and 17, the rate of pressure is decreased and increased respectively with blend ratio of 5:95. At zero degree crank angle and CR of 16 (for 5% TO), 17 (for 10% TO), 16 (for 10% TO), 15 (for 5% TO), and 17.5 (for 10% TO), the pressure rate is calculated as 3.6, 3.3, 1.5, 2 and 3.2 respectively. Negative peak arises for the rate of pressure parameter in all CRs and it has no unit. The parameter mass fraction burned is calculated and for 10% blend with CR16, it is found to be higher at 150° crank angle when compared with the other curves. At CR of 17.5 and blend ratio 5:95, the fuel line pressure is more at pressure of 35 bars, that is very high than the fuel line pressure in CR 16. The cylinder pressure is noted as 51 bar with a sharp peak at 25° crank angle for CR 17.5 (in 5% TO-diesel blend) and 15. It is also found that

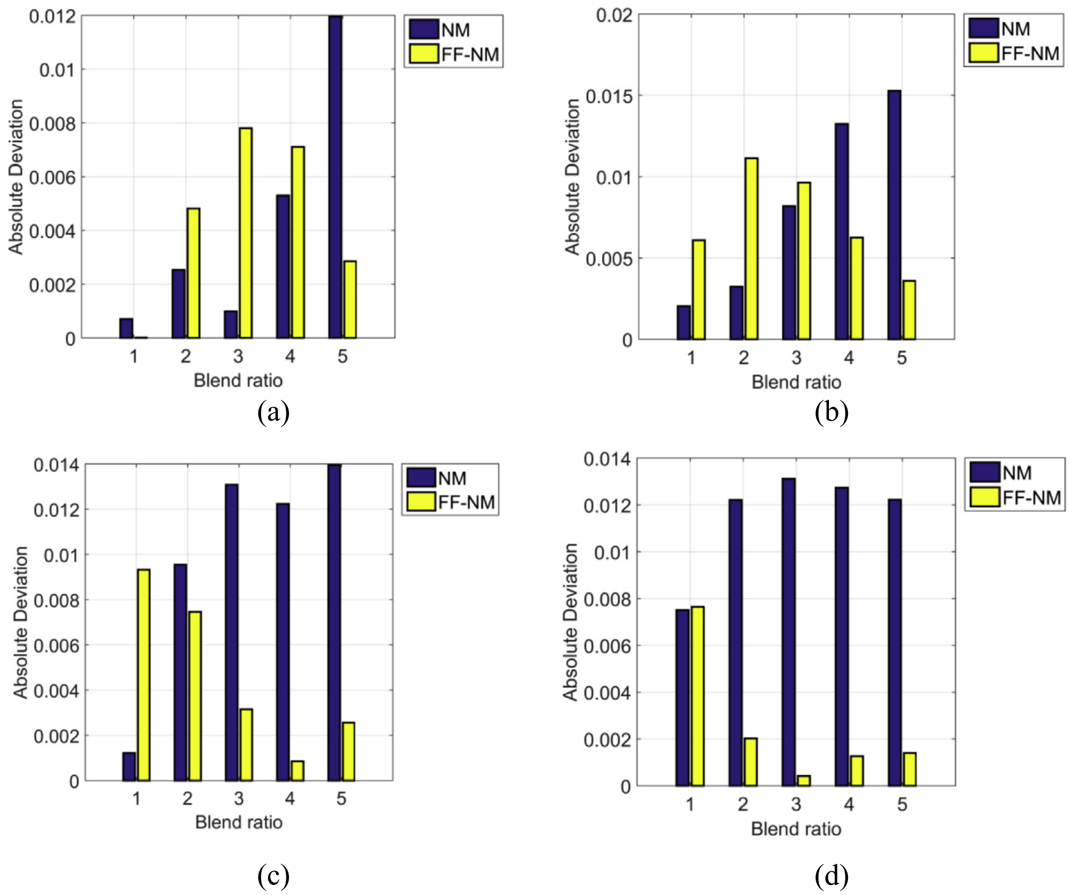

Fig. 11. Absolute deviation of miniature blends of CO for the proposed FF-NM method over NM method under varying compression ratios of (a) 15, (b) 16, (c) 17, (d) 17.5.

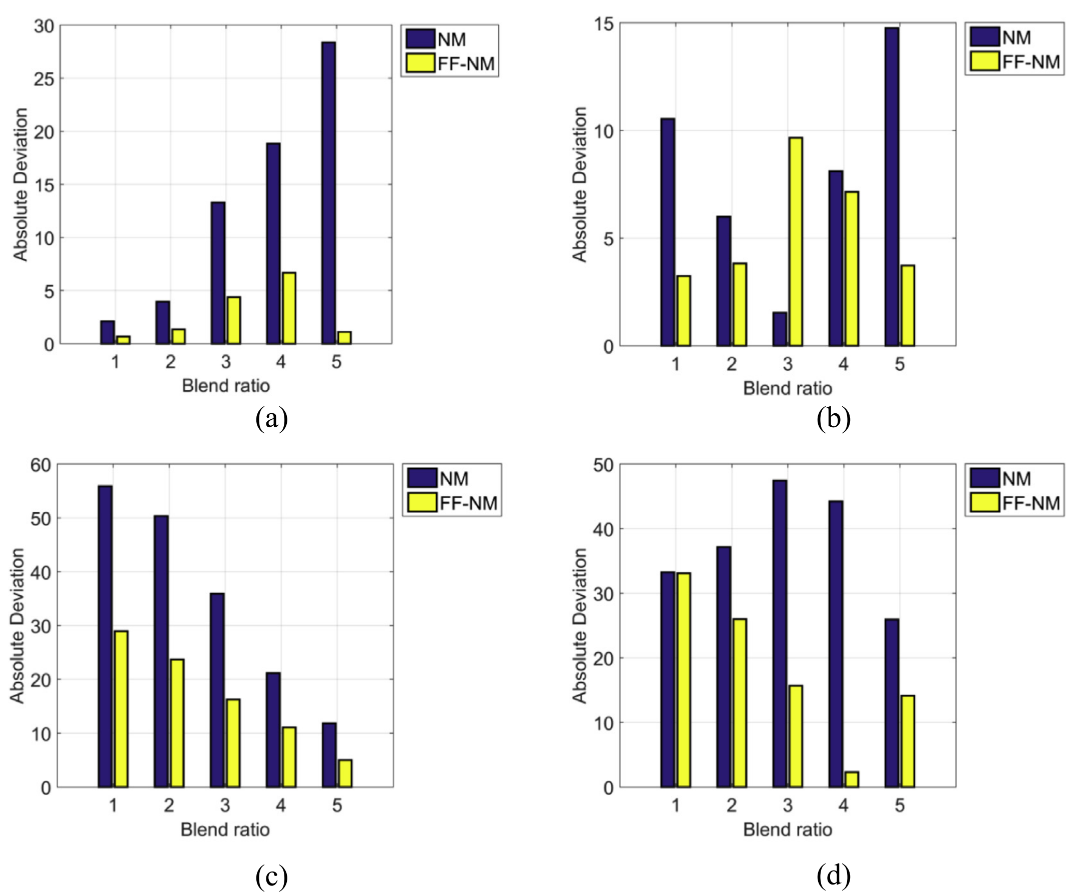

Fig. 12. Absolute deviation of miniature blends of NO_x for the proposed FF-NM method over NM method under varying compression ratios of (a) 15, (b) 16, (c) 17, (d) 17.5.

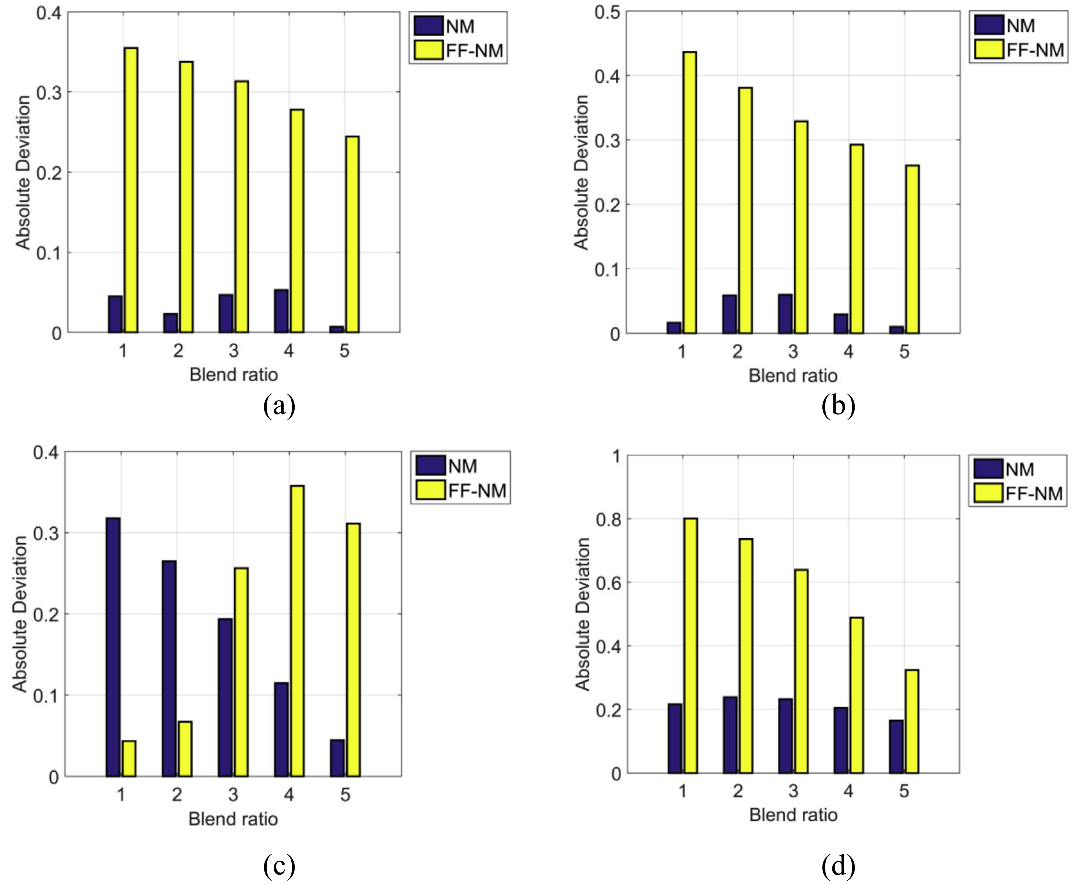

Fig. 13. Absolute deviation of miniature blends of O_2 for the proposed FF-NM method over NM method under varying compression ratios of (a) 15, (b) 16, (c) 17, (d) 17.5.

the peak exists for all compression ratios. In CR15 with blend ratio 5:95, the cumulative heat release rate, calculated in kJ is more with sharp peak. In addition, the net heat release rate is estimated in J/deg at different CRs and the values are in peak at 18(at 0°), 18 (at 25°), 35 (at 0°), 33(at 0°), 30(at 0°), 25(at 50°), 18(at 0°), with CRs of 16(for 10% TO), 15(for 5% TO), 17(for 10% TO), 17(for 5% TO), 17.5(for 5% TO), 17.5(for 10% TO), and 15 (for 10% TO), respectively.

5. Model performance

The emission of CO_2, CO, HC, O_2 and NO_x, when the TO-diesel blends in the ratio of 6%, 7%, 8%, 9%, 10% at different CRs 15, 16, 17, 17.5 is analysed for the actual, NM and the FF-NM method and they are graphically illustrated in Figs. 4–8 respectively. It is noticed that in the CO_2 emission analysis, as per Fig. 4, the FF-NM curve shows 0.7%, 0.05% closer to the actual curve than the NM at CR15 and 17.5 respectively, though the NM predicts the actual value as close as possible.

In the analysis of CO emission, as given in Fig. 6, the FF-NM plot shows 0.0125%, 0.01%, 0.01% and 0.01% closer than the NM at CR of 15, 16, 17 and 17.5 respectively. The estimated precision value of HC emission, as given in Fig. 5, shows that the FF-NM almost estimates the actual HC emission and it is closer than the estimation from NM. Such results can be observed for all the variants of CR, except 17.5. Similarly in Fig. 7, where the estimation results of O_2 emission is presented, the deviation between the actual and the estimated results from FF-NM lesser than the estimation from NM. Such improvement of the FF-NM over NM has been reported as 25%, 10%, 10% and 8% for the CR of 15, 16, 17 and 17.5, respectively. The similar kind of performance improvement has been exhibited by FF-NM in estimating the NO_x emission with no exemption on any variants, as per Fig. 8.

The performance deviation of miniature blends of CO_2, HC, CO, NO_x and O_2 for the proposed FF-NM method over NM method under the respective varying compression ratio of 15, 16, 17 and 17.5 are shown in Figs. 9–13 respectively. The average error deviation performance of proposed FF-NM method on analysing different emission gases is lesser than the NM method under varying compression ratios except in a few instance of Fig. 9(b) and (c), 10 (a) and (d), 13 (a), (b) and (d) where it shows the maximum average error deviation over NM method. Fig. 14 represents the real experimental set up. Table 4 represents the computational complexity of existing and proposed model.

6. Concluding remarks

In recent years, the biofuels are utilized mostly because of its renewable capacity. The environment gets contaminated due to the emission of GHG and other toxic gases from the diesel engine of vehicles. Researchers put attention to minimize the release of poisonous gases that cause lot of side effects to the environment and developed new methodologies. The present paper addressed the problems with respect to the use of conventional fuel-diesel and introduced the Tamanu oil-diesel oil blend with different compression ratios 15, 16, 17, 17.5 and blend ratios 5:95, 6:94, 7:93, 8:92, 9:91 and 10:90. A new modeling method called FF-NM is proposed and the engine performance and emission analysis of the TO-diesel oil blend has been evaluated and compared with the

Fig. 14. Real experimental set up.

Table 4
Computational complexity of existing and proposed model.

Model	NM	FF-NM
CR15	3.0333	1.3648
CR16	3.1235	1.2345
CR17	3.4567	1.2367
CR17.5	1.2467	1.6345

actual and NM, which is our previous modeling technique, outcomes. The MSE is determined for both the modeling methods and they are found to be lesser for all the predicted parameters with respect to varying blend ratios and CRs compared to the NM method. The emission characteristics of CO_2, CO, HC, NO_x and O_2 at different CRs for the actual, NM and FF-NM have been calculated with the selected blend ratios and it has been identified that the estimation errors in FF-NM method of all GHG were lesser than the NM method. The evaluated results show good performance of the proposed FF-NM method.

References

[1] B.J. Bora, U.K. Saha, Experimental evaluation of a rice bran biodiesel − biogas run dual fuel diesel engine at varying compression ratios, Renew. Energy 87

(no. 1) (March 2016) 782–790.
[2] B.J. Bora, U.K. Saha, Optimisation of injection timing and compression ratio of a raw biogas powered dual fuel diesel engine, Appl. Therm. Eng. 92 (January 2016) 111–121.
[3] S. Nagaraja, K. Sooryaprakash, R. Sudhakaran, Investigate the effect of compression ratio over the performance and emission characteristics of variable compression ratio engine fueled with preheated palm oil - diesel blends, Procedia Earth Planet. Sci. 11 (2015) 393–401.
[4] V. Gnanamoorthi, G. Devaradjane, Effect of compression ratio on the performance, combustion and emission of DI diesel engine fueled with ethanol – Dieselblend, J. Energy Inst. (2014) 1–8.
[5] R. Senthil, R. Silambarasan, N. Ravichandiran, "Influence of injection timing and compression ratio on performance, emission and combustion characteristics of Annona methyl ester operated diesel engine, Alexandria Eng. J. 54 (no. 3) (September 2015) 295–302.
[6] T.A. Kumar, R. Chandramouli, T. Mohanraj, A study on the performance and emission characteristics of esterified pinnai oil tested in VCR engine, Ecotoxicol. Environ. Saf. 121 (November 2015) 51–56.
[7] V.S. Selvabala, D.K. Selvaraj, J. Kalimuthu, P.M. Periyaraman, S. Subramanian, Two-step biodiesel production from Calophyllum inophyllum oil: optimization of modified β-zeolite catalyzed pre-treatment, Bioresour. Technol. 102 (no. 2) (January 2011) 1066–1072.
[8] I.M.R. Fattah, H.H. Masjuki, M.A. Kalam, M.A. Wakil, A.M. Ashraful, S.A. Shahir, Experimental investigation of performance and regulated emissions of a diesel engine with Calophyllum inophyllum biodiesel blends accompanied by oxidation inhibitors, Energy Conserv. Manag. 83 (July 2014) 232–240.
[9] B.R.R. Bapu, L. Saravanakumar, B.D. Prasad, Effects of combustion chamber geometry on combustion characteristics of a DI diesel engine fueled with calophyllum inophyllum methyl ester, J. Energy Inst. 90 (1) (February 2017) 82–100.
[10] N. Muthukumaran, C.G. Saravanan, S.P.R. Yadav, R. Vallinayagam, S. Vedharaj, W.L. Roberts, Synthesis of cracked Calophyllum inophyllum oil using fly ash catalyst for diesel engine application, Fuel 155 (September 2015) 68–76.
[11] N.S. Kitakawa, H. Honda, H. Kuribayashi, T. Toda, T. Fukumura, T. Yonemoto, Biodiesel production using anionic ion-exchange resin as heterogeneous catalyst, Bioresour. Technol. 98 (no. 2) (January 2007) 416–421.
[12] N.U. Soriano, R. Venditti, D.S. Argyropoulos, Biodiesel synthesis via homogeneous lewis acid-catalyzed transesterification, Fuel 88 (no. 3) (March 2008) 560–565.
[13] L.C. Meher, S. Vidya, S. Dharmagadda, S.N. Naik, Optimization of alkali catalyzed transesterification of Pongamia pinnata oil for production of biodiesel, Bioresour. Technol. 97 (August 2006) 1392–1397.
[14] B.K. Venkanna, C.V. Reddy, Biodiesel production and optimization from Calophyllum inophyllum linn oil (honne oil) – a three stage method, Bioresour. Technol. 100 (November 2009) 5122–5125.
[15] J. Kansedo, K.T. Lee, S. Bhatia, Biodiesel production from palm oil via heterogeneous transesterification, Biomass Bioenergy 33 (February 2008) 271–276.
[16] G. Knothe, L.F. Razon, F.T. Bacani, Kenaf oil methyl esters, Ind. Crop. Prod. 49 (August 2013) 568–572.
[17] A.M. Ashraful, H.H. Masjuki, M.A. Kalam, I.M.R. Fattah, S. Imtenan, S.A. Shahir, et al., Production and comparison of fuel properties, engine performance, and emission characteristics of biodiesel from various non-edible vegetable oils: a review, Energy Convers. Manag. 80 (April 2014) 202–228.
[18] A.E. Atabani, A.S. Silitonga, H.C. Ong, T.M.I. Mahlia, H.H. Masjuki, I.A. Badruddin, et al., Non-edible vegetable oils: a critical evaluation of oil extraction, fatty acid compositions, biodiesel production, characteristics, engine performance and emissions production, Renew. Sustain. Energy Rev. 18 (February 2013) 211–245.
[19] M. Serrano, A. Bouaid, M. Martínez, J. Aracil, Oxidation stability of biodiesel from different feedstocks: influence of commercial additives and purification step, Fuel 113 (November 2013) 50–58.
[20] A. Obadiah, R. Kannan, A. Ramasubbu, S.V. Kumar, Studies on the effect of antioxidants on the long-term storage and oxidation stability of Pongamia pinnata (L.) Pierre biodiesel, Fuel Process. Technol. 99 (July 2012) 56–63.
[21] X.S. Yang, Nature-inspired Metaheuristic Algorithms, Luniver Press, UK, 2008.
[22] X.S. Yang, Firefly algorithms for multimodal optimisation, in: Proc. 5th Symposium on Stochastic Algorithms, vol. 5792, Foundations and Applications, 2009, pp. 169–178.
[23] H.P. Gavin, The Levenberg-marquardt Method for Nonlinear Least Squares Curve-fitting Problems, 2016.
[24] X. He, X.S. Yang, Firefly algorithm: recent advances and applications, Int. J. Swarm Intell. 1 (no.1) (2013) 36–50.
[25] Jiamei Deng, Richard Stobart, Maass, Bastian, The applications of artificial neural networks to engines, Artif. Neural Network- Ind. Contr. Eng. Appl. (April 2011) 309–332.